

Semi-transparent thermo-electric cells based on bismuth telluride and its composites with CNTs and graphene

NOSHIN FATIMA^a, Kh. S. KARIMOV^{a,b}, JAMEEL-UN NABI^a, HONG MENG^c, ZUBAIR AHMAD^{d,*}, M. RIAZ^a, M. MEHRAN BASHIR^a, M. IMRAN KHAN^a, RASHID ALI^a, ADAM KHAN^e, FARID TOUATI^f

^a*Ghulam Ishak Khan Institute of Engineering Science and Technology, Topi, 23640, Swabi, KPK, Pakistan.*

^b*Center for Innovative Development of Science and New Technologies of Academy of Sciences, Rudaki Ave.33, Dushanbe, 734025, Tajikistan.*

^c*School of Advanced Materials, Peking University Shenzhen Graduate School, Peking University, Shenzhen 518055, China*

^d*Center for Advanced Materials (CAM), Qatar University, P. O.Box 2713, Doha, Qatar*

^e*Department of Electronics Engineering UET Peshawar (Abbottabad Campus), KPK, Pakistan.*

^f*Department of Electrical Engineering, College of Engineering, Qatar University, P. O.Box 2713, Doha, Qatar*

In this paper, semi-transparent thin film thermo-electric cells based on the composite of bismuth telluride (Bi_2Te_3 , p-type and n-type) with graphene and carbon nanotubes (CNTs) have been reported. The voltage, current and Seebeck effect have been measured as a function of the temperature gradient. It was found that the addition of the CNTs and graphene in the Bi_2Te_3 matrix increase the thermo-electric current and the thermo-electric voltage of the Bi_2Te_3 based control cells. The thermo-electric performance of the $\text{Bi}_2\text{Te}_3/\text{CNTs}$ composite was found to be superior as compared to the $\text{Bi}_2\text{Te}_3/\text{graphene}$ composite. Furthermore, the addition of the CNTs or graphene in n- Bi_2Te_3 showed better improvement in thermo-electric properties as compared to their composite with p- Bi_2Te_3 . Potentially, the semitransparent thermo-electric cells can be used for fabrication of special windows which can produce the electric power due to the temperature gradient.

(Received June 19, 2018; accepted June 14, 2019)

Keywords: Bismuth telluride, Graphene, CNTs, Seebeck coefficient, Temperature-gradient, Semitransparent thermo-electric cell, Polymer adhesive

1. Introduction

The latest promising trend in renewable energy is the use of semitransparent devices. The semitransparent concept is very common in solar cells and this area of technology has attained a significant interest in the last few years. However, the research on the semitransparent thermo-electric cells, in particular, is still at an early stage, despite its future seems to be very bright due to recent trends and technological advantages of the transparent cells. Simultaneously, it is important to note that the fabrication of semitransparent thermo-electric cells is entirely different than semitransparent solar cells due to the different working principle, their structure and fabrication technology [1, 2]. The thermo-electric cells are working on the base of the Seebeck effect [3]. Thermo-electric efficiency is determined by the Seebeck coefficient (α), electrical conductivity (σ) and total thermal conductivity ($K_{tot} = K_{el} + K_{ph}$) which is equal to the sum of the electron (K_{el}) and phonon (K_{ph}) thermal conductivities [4]. The efficiency of a thermo-electric generators strongly depends upon the phonon thermal conductivity (K_{ph}).

The Seebeck voltage (or coefficient (α)) depends on the material type [5, 6]. In extrinsic semiconductors (p-type and n-type), the value of Seebeck voltage is higher (200-1000 $\mu\text{V}^\circ\text{C}^{-1}$) than in intrinsic semiconductors and decreases when temperature increases. In metals or conductors, Seebeck voltage is quite lower (0-60 $\mu\text{V}^\circ\text{C}^{-1}$) and slowly

increases with rise in temperature. However, Seebeck coefficient is found to be higher in quasi-one-dimensional organic semiconductor crystals (around of 500-1000 $\mu\text{V}^\circ\text{C}^{-1}$) [6]. The value of α can be increased while the k_{tot} can be reduced by controlling the structures of the thermo-electric materials.

As far as the materials for thermo-electric cells are concerned, bismuth telluride (Bi_2Te_3) and its alloys have been widely investigated. For instance, in [7], the authors fabricated Bi_2Te_3 nanostructures for low-temperature thermoelectric applications. In [8], the Bi_2Te_3 nanoparticles were synthesized and these nanoparticles exhibit higher Seebeck coefficient ($-135\mu\text{VK}^{-1}$) and lower thermal conductivity (0.957 W(mK)^{-1}). Bulk nanostructured based undoped Bi_2Te_3 is reported in [9] to have a Seebeck coefficient of $-120\mu\text{VK}^{-1}$. In [10], n-type nanocrystalline bismuth-telluride based thin films were investigated and achieved a Seebeck coefficient of $-186.1\mu\text{VK}^{-1}$. Similarly, Michez et al. [11] reported the bismuth telluride (Bi_2Te_3)- Sb_2Te_3 (p-type) and Bi_2Te_3 - Bi_2Se_3 (n-type) with high figure of merit (ZT). Thermo-electric properties of graphene [12-14] and CNTs [15-17] have also investigated in a number of papers. Nano-structuring and bandgap engineering of graphene can reduce the lattice thermal conductance and enhance the Seebeck coefficient. CNTs filled composites used for thermo-electric generators typically offer superior potential where the CNTs increase the power factor with increasing temperature [18].

Keep in view, the potential of Bi_2Te_3 , graphene and CNTs for the thermo-electric devices, in this paper, we presented a successful attempt to design semitransparent thermo-electric cells, for conversion of thermal energy into electric energy using the composite of Bi_2Te_3 with CNTs and graphene. Considering the potential advantages of the semitransparent power generating devices, the new design (a hollow cylindrical semitransparent) of the thermo-electric cells has been presented. The proposed semitransparent cells can be used in special windows to produce the electric power due to the temperature gradient and at the same time, transmitted light can be used to illuminate the rooms or house.

2. Experimental

For the fabrication of thermo-electric cells, commercially available p-type bismuth Telluride ($\text{p-Bi}_2\text{Te}_3$) and n-type bismuth Telluride ($\text{n-Bi}_2\text{Te}_3$) powders were used. The average sizes of the particles were around $11.56 \mu\text{m}$ and $12.15 \mu\text{m}$ for n- Bi_2Te_3 and p- Bi_2Te_3 , respectively. There were six different composites prepared for three sets of devices. For the first set, the composites were made by

mixing the n- Bi_2Te_3 and p- Bi_2Te_3 with 30 wt.% commercially available polymer (GMSA) adhesive. Whereas in the second set, 5wt.% of CNTs powder was added to p- Bi_2Te_3 and n- Bi_2Te_3 adhesive composites and in the third set 5wt. % of graphene was added to p- Bi_2Te_3 and n- Bi_2Te_3 adhesive composites.

For the fabrication of the semitransparent thermo-electric cells, $100 \mu\text{m}$ thick layers of the prepared composites were deposited on the outer surface of hollow glass cylindrical substrates. The cells were kept to dry for overnight. The outer and internal diameters and height of the cylindrical substrate were 10 mm, 8 mm and 10 mm, respectively. The transparency of the composite films was in the range of 32-35%. Cylindrical metal rings were fixed as electrodes on the top and bottom edges of the cylindrical substrates. Schematic diagrams of the cross-sectional and top views of the thermo-electric cells are shown in Fig. 1 (a) and (b), respectively. The miniature heaters were attached at both ends of cells to create the gradient of temperature. This gradient of temperature was measured by Fluke 87 multi-meters attached with thermocouples at the metallic electrodes in Figs. 1 (a), 3 and 4. Current and voltage was measured by the HIOKI-DT4253 digital multi-meter.

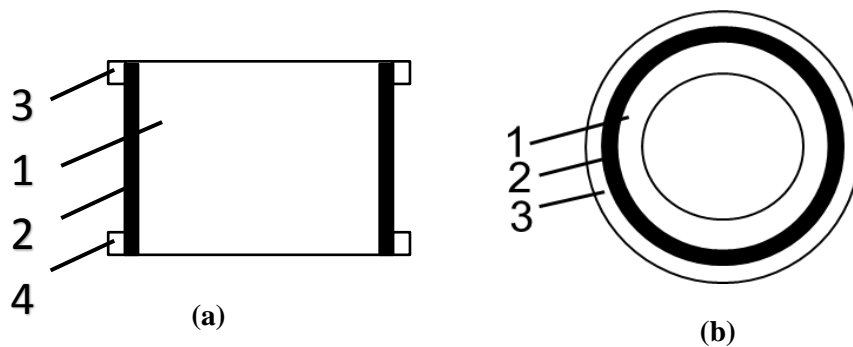


Fig. 1. Schematic diagram of thermo-electric cell: cross-sectional view (a) and top view (b): cylindrical body (1), thermo-electric material (Bi_2Te_3 composite) (2), metallic electrodes (3 and 4)

Fig. 2 shows X-ray diffraction (XRD) graphs of the n- Bi_2Te_3 and p- Bi_2Te_3 samples. X-ray diffraction of the samples was conducted with Philips PW1830 powder X-ray diffraction system in Bragg-Brentano (θ - 2θ) scan mode using $\text{Cu-K}\alpha$ radiation source. In the diffractograms, the peak of bismuth telluride (n-type) was observed at 2θ of 27.87° (Fig. 2 (a)), which is consistent with standard XRD data (PDF 051-0643) [19]. On the other hand, the peak of bismuth telluride (p-type) was observed at 2θ of 28.11° (Fig. 2 (b)), which is also consistent with standard XRD data (PDF 049-1713) [19].

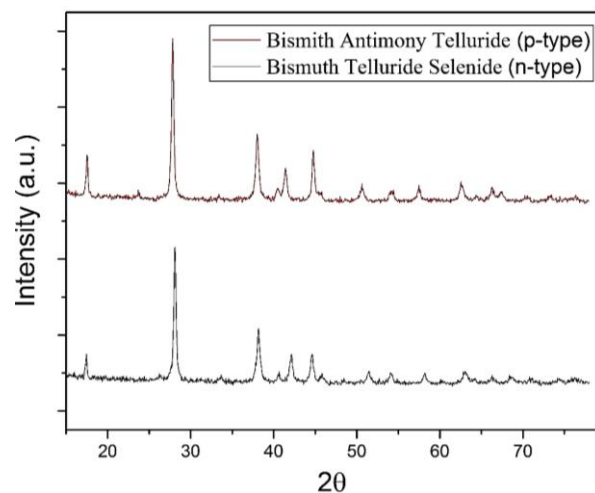


Fig. 2. X-ray diffraction pattern of bismuth telluride selenide (n-type) powder sample and bismuth antimony telluride (p-type) powder sample

3. Results and discussions

The Seebeck effect vs. temperature relationship for the p-type and n-type Bi_2Te_3 and their composites with graphene and CNTs are shown in Figure 3 and 4. Obviously, the addition of CNTs or graphene to the Bi_2Te_3 increases the thermo-electric current and thermo-electric voltage. The CNTs based samples produce higher current and voltages as compared to the graphene, which, probably, due to the higher electrical conductivity of the CNTs with respect to graphene. The increase of the conductivity due to the presence of CNTs or graphene decreases the internal electrical resistance of the samples, that in turn increases the short-circuit current which was observed experimentally. The increase in the thermo-electric voltage can be explained by the increase of the mobility of charge carriers between Bi_2Te_3 particles due to a decrease of potential barriers owing to the presence of CNTs or graphene particles. Also, it is observed that the addition of CNTs or graphene into n- Bi_2Te_3 has improved its thermo-electric properties more than that of p- Bi_2Te_3 . Even though, the Seebeck coefficient of CNTs-adhesive (10-35) $\mu\text{V}/^\circ\text{C}$ and graphene-adhesive (15-50) $\mu\text{V}/^\circ\text{C}$ in the temperature range of 25-70 $^\circ\text{C}$, the presence of CNTs or graphene in the Bi_2Te_3 decreases internal resistances compared to the p- Bi_2Te_3 or n- Bi_2Te_3 samples alone. These results are summarized in Table I. The internal resistances of the samples were calculated as the ratio of the open-circuit voltage to short-circuit current and found to be: 12.5 k Ω (p- Bi_2Te_3), 4.16 k Ω (n- Bi_2Te_3), 1.87 k Ω (p- Bi_2Te_3 -CNTs), 6.87 k Ω (n- Bi_2Te_3 -CNTs), 1.56 k Ω (p- Bi_2Te_3 -graphene), and 5.33 k Ω (n- Bi_2Te_3 -graphene).

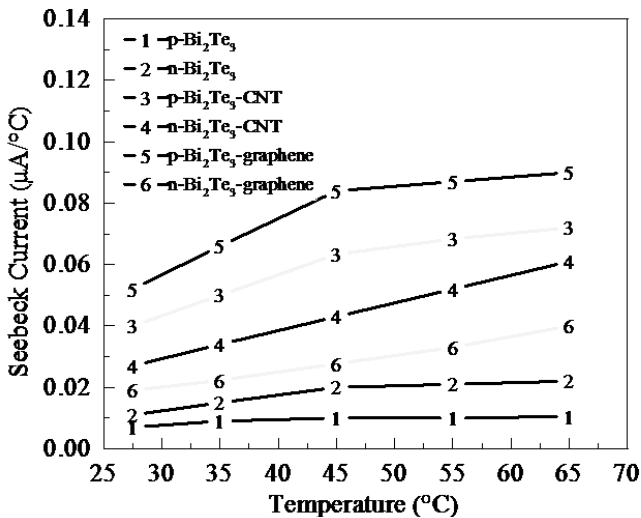


Fig. 3. Seebeck effect of short-circuit current vs. temperature relationships for the Bi_2Te_3 and its composites

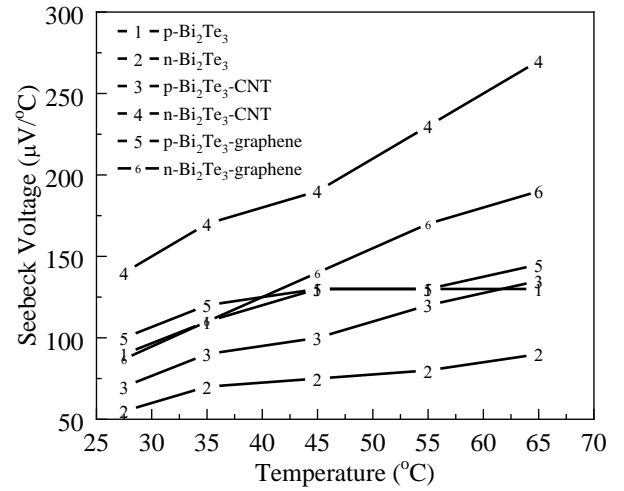


Fig. 4. Seebeck effect of open-circuit voltage vs. temperature relationships for the Bi_2Te_3 its composites

The performance of a thermo-electric cell is judged by a dimensionless quantity known as the figure of merit (ZT) [20]. A larger ZT value indicates a higher thermodynamic efficiency. More specifically, the ZT is used to compare the potential efficiency of devices using different thermo-electric materials. A $ZT = 1$, is considered as good; however, to compete with other energy harvesting device values in the range of 3-4 are essential. To date, the best reported ZT values are ~ 2 [21-23]. The efficiency of a thermo-electric cell can be determined by [24]:

$$\eta_{max} = \frac{T_H - T_C}{T_H} \frac{\sqrt{1 + Z\bar{T}} - 1}{\sqrt{1 + Z\bar{T}} + \frac{T_C}{T_H}} \quad (1)$$

where, T_H is the temperature at the hot junction and T_C is the temperature at the surface being cooled. $Z\bar{T}$ is the modified dimensionless figure of merit (considering the thermo-electric capacity of both thermo-electric materials being used in the device). Using the experimental data, we found η to be around 1.8% for n- Bi_2Te_3 and p- Bi_2Te_3 , and 2.2% for n- Bi_2Te_3 -CNTs-adhesive and p- Bi_2Te_3 -CNTs-adhesive at a temperature gradient of 10 $^\circ\text{C}$. These experimental values of the efficiency are close to the theoretical values calculated using Eq. 1. For practical applications of thermo-electric cells and generators, the temperature gradient between hot and cold terminals should be increased as much as practically possible.

Figs. 5 and 6 shows the short-circuit current and the open-circuit voltage as a function of the temperature for p-type and n-type Bi_2Te_3 and their composites with graphene and CNTs. The increase in short-circuit current at $T = 65$ $^\circ\text{C}$ in p- Bi_2Te_3 , n- Bi_2Te_3 , p- Bi_2Te_3 +CNTs, n- Bi_2Te_3 +CNTs, p- Bi_2Te_3 +graphene and n- Bi_2Te_3 +graphene is found to be 1.5, 2, 1.75, 2.26, 1.73 and 2.1 times, respectively, for a cold terminal temperature $T = 27$ $^\circ\text{C}$. This corresponds to an increase in voltage of 1.44, 1.64, 1.85, 1.93, 1.45 and 2.18 times, respectively. These results show that highest increases in currents and voltages are observed for n- Bi_2Te_3 +CNTs and n- Bi_2Te_3 +graphene composites.

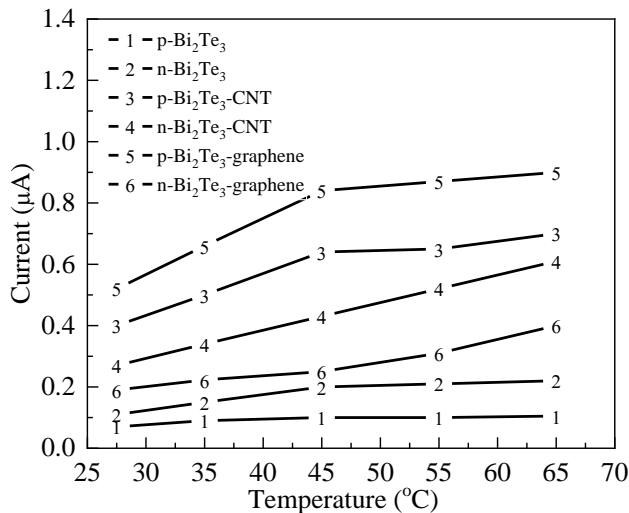


Fig. 5. Short-circuit current vs. average temperature relationships for the Bi_2Te_3 and its composites

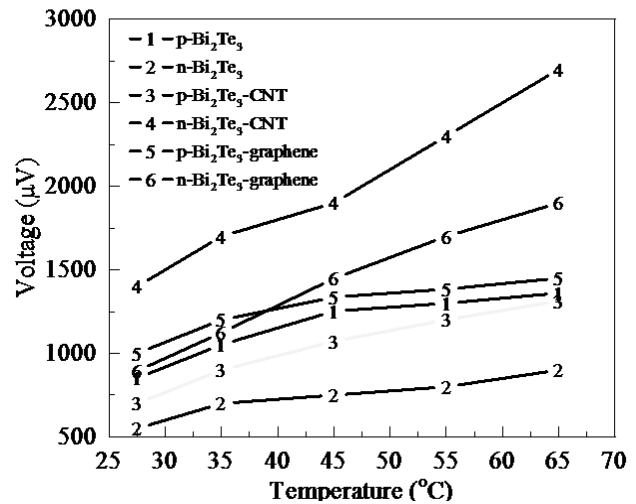


Fig. 6. Open-circuit voltage vs. average temperature relationships for the Bi_2Te_3 and its composites

Table 1. Summary of Bi_2Te_3 composites thermo-electric properties (at temperature gradient $\sim 10^\circ\text{C}$)

Thin Film	Increase in current	Increase in voltage
p- Bi_2Te_3	1.5	1.44
n- Bi_2Te_3	2	1.64
p- Bi_2Te_3 +CNTs	1.75	1.85
n- Bi_2Te_3 +CNTs	2.26	1.93
p- Bi_2Te_3 +graphene	1.73	1.45
n- Bi_2Te_3 +graphene	2.1	2.18

4. Conclusion

In this paper, we have reported the design and fabrication of hollow cylindrical semitransparent thermoelectric cells based on the p- Bi_2Te_3 , n- Bi_2Te_3 and their composites with CNTs and graphene composite films. With the increase in average temperature, the current and voltage of the thermo-electric cells increases. These results show that highest increases in currents and voltages are observed for n- Bi_2Te_3 +CNTs and n- Bi_2Te_3 +graphene composites whereas the lowest resistance was found in p- Bi_2Te_3 - graphene composite.

Acknowledgements

The authors are thankful to the Ghulam Ishaq Khan Institute of Engineering Sciences and Technology and HEC of Pakistan for the supporting this work.

References

- [1] M. Sumino, K. Harada, M. Ikeda, S. Tanaka, K. Miyazaki, C. Adachi, Applied Physics Letters **99**, 188 (2011).
- [2] B. Sb, Nanostructured Thermoelectric Materials, Modules, Systems, and Applications in Thermoelectrics, 2 (2012).
- [3] L. E. Bell, Science **321**, 1457 (2008).
- [4] N. Chen, F. Gascoin, G. J. Snyder, E. Müller, G. Karpinski, C. Stiewe, Applied Physics Letters **87**, 171903 (2005).
- [5] P.-H. Chang, M. S. Bahramy, N. Nagaosa, B. K. Nikolic, Nano Letters **14**, 3779 (2014).
- [6] M. Zeng, W. Huang, G. Liang, Nanoscale **5**, 200 (2013).
- [7] V. Akshay, M. Suneesh, M. Vasundhara, Inorganic Chemistry **56**, 6264 (2017).
- [8] S. Pradhan, R. Das, R. Bhar, R. Bandyopadhyay, P. Pramanik, Journal of Nanoparticle Research **19**, 69 (2017).
- [9] M. Saleemi, M. S. Toprak, S. Li, M. Johnsson, M. Muhammed, Journal of Materials Chemistry **22**, 725 (2012).
- [10] M. Takashiri, K. Miyazaki, S. Tanaka, J. Kurosaki, D. Nagai, H. Tsukamoto, Journal of Applied Physics **104**, 084302 (2008).
- [11] A. Michez, A. Giani, A. Boyer, A. Foucaran, Sensors and Actuators A: Physical **107**, 36 (2003).

- [12] X. Zhang, L.-D. Zhao, *Journal of Materiomics* **1**, 92 (2015).
- [13] G. Chen, D. Kraemer, A. Muto, K. McEnaney, H.-P. Feng, W.-S. Liu, Q. Zhang, B. Yu, Z. Ren, *SPIE Proceedings* **8031**, 80311J (2011).
- [14] D. Dong, H. Guo, G. Li, L. Yan, X. Zhang, W. Song, *Nano Energy* **39**, 470 (2017).
- [15] R. Hu, B. A. Cola, N. Haram, J. N. Barisci, S. Lee, S. Stoughton, G. Wallace, C. Too, M. Thomas, A. Gestos, *Nano letters* **10**, 838 (2010).
- [16] M. He, F. Qiu, Z. Lin, *Energy & Environmental Science* **6**, 1352 (2013).
- [17] T. Luo, K. Pan, Flexible Thermoelectric Device Based on Poly (ether-b-amide12) and High-purity Carbon Nanotubes Mixed Bilayer Heterogeneous Films, *ACS Applied Energy Materials*, DOI (2018).
- [18] X. Zhou, C. Pan, A. Liang, L. Wang, W.-Y. Wong, *Composites Science and Technology* **145**, 40 (2017).
- [19] A. Minnich, M. Dresselhaus, Z. Ren, G. Chen, *Energy & Environmental Science* **2**, 466 (2009).
- [20] A. Bulusu, D. Walker, *Superlattices and Microstructures* **44**, 1 (2008).
- [21] K. F. Hsu, S. Loo, F. Guo, W. Chen, J. S. Dyck, C. Uher, T. Hogan, E. Polychroniadis, M. G. Kanatzidis, *Science* **303**, 818 (2004).
- [22] K. Biswas, J. He, I. D. Blum, C.-I. Wu, T. P. Hogan, D. N. Seidman, V. P. Dravid, M. G. Kanatzidis, *Nature* **489**, 414 (2012).
- [23] D. Dragoman, M. Dragoman, *Applied Physics Letters* **91**, 203116 (2007).
- [24] X. Ni, G. Liang, J.-S. Wang, B. Li, *Applied Physics Letters* **95**, 192114 (2009).

*Corresponding author: zubairtarar@qu.edu.qa